



## Article

# Carbon-Isovalent Dopant Pairs in Silicon: A Density Functional Theory Study

Stavros-Richard G. Christopoulos <sup>1,2</sup> , Efstratia N. Sgourou <sup>3</sup>, Alexander Chroneos <sup>4,5,\*</sup>   
and Charalampos A. Londos <sup>3</sup>

<sup>1</sup> Department of Computer Science, School of Computing and Engineering, University of Huddersfield, Huddersfield HD1 3DH, UK

<sup>2</sup> Centre for Computational Science and Mathematical Modelling, Coventry University, Coventry CV1 2TU, UK

<sup>3</sup> Physics Department, Solid State Physics Section, National and Kapodistrian University of Athens, Panepistimiopolis Zografos, 15784 Athens, Greece; e\_sgourou@hotmail.com (E.N.S.); hlontos@gmail.com (C.A.L.)

<sup>4</sup> Department of Electrical and Computer Engineering, University of Thessaly, 38221 Volos, Greece

<sup>5</sup> Department of Materials, Imperial College London, London SW7 2BP, UK

\* Correspondence: alexander.chroneos@imperial.ac.uk; Tel.: +30-6978775320

**Abstract:** Carbon (C) is an important isovalent impurity in silicon (Si) that is inadvertently added in the lattice during growth. Germanium (Ge), tin (Sn), and lead (Pb) are isovalent atoms that are added in Si to improve its radiation hardness, which is important for microelectronics in space or radiation environments and near reactors or medical devices. In this work, we have employed density functional theory (DFT) calculations to study the structure and energetics of carbon substitutional-isovalent dopant substitutional  $C_sD_s$  (i.e.,  $C_sGe_s$ ,  $C_sSn_s$  and  $C_sPb_s$ ) and carbon interstitial-isovalent dopant substitutional  $C_iD_s$  (i.e.,  $C_iGe_s$ ,  $C_iSn_s$  and  $C_iPb_s$ ) defect pairs in Si. All these defect pairs are predicted to be bound with the larger isovalent atoms, forming stronger pairs with the carbon atoms. It is calculated that the larger the dopant, the more stable the defect pair, whereas the  $C_sD_s$  defects are more bound than the  $C_iD_s$  defects.

**Keywords:** silicon; nitrogen; intrinsic defects



**Citation:** Christopoulos, S.-R.G.; Sgourou, E.N.; Chroneos, A.; Londos, C.A. Carbon-Isovalent Dopant Pairs in Silicon: A Density Functional Theory Study. *Appl. Sci.* **2024**, *14*, 4194. <https://doi.org/10.3390/app14104194>

Received: 25 April 2024

Revised: 13 May 2024

Accepted: 14 May 2024

Published: 15 May 2024



**Copyright:** © 2024 by the authors. Licensee MDPI, Basel, Switzerland. This article is an open access article distributed under the terms and conditions of the Creative Commons Attribution (CC BY) license (<https://creativecommons.org/licenses/by/4.0/>).

## 1. Introduction

Silicon (Si) is the key semiconductor for integrated circuits, transistors, sensors, detectors, solar cells, as well as for applications related to nuclear medicine, space industry, telecommunications, and quantum computing [1–5]. An important issue in the performance of the devices is the presence of defects which affect their electrical, optical, and mechanical properties [6–9]. Obviously, it is significant to understand the behavior of the defects in order to control the performance of the devices, either by suppressing their detrimental effects or by enhancing their beneficial influence in the material. Thus, by proper defect engineering, we can enhance the efficiency of the material for certain applications.

The main isovalent impurities in silicon, that is C, Ge, Sn, and Pb, play an important role as their presence in the lattice influence the material's properties. Ge, Sn, and Pb occupy substitutional sites in the Si lattice, and since they are electrically inactive, they do not affect the electrical behavior of the material. Additionally, due to the difference in the covalent radius ( $r_C = 0.77 \text{ \AA}$ ,  $r_{Ge} = 1.22 \text{ \AA}$ ,  $r_{Sn} = 1.41 \text{ \AA}$ ,  $r_{Pb} = 1.44 \text{ \AA}$ ) compared to that of Si, ( $r_{Si} = 1.17 \text{ \AA}$ ), they give rise to local elastic strains which can affect the equilibrium between the concentrations of vacancies and self-interstitials, and the interactions between them as well as with other impurities present. Indeed, Ge, Sn, and Pb, which are bigger than Si and therefore introduce compressive strains in the lattice, tend to associate with vacancies; however, C, which is smaller than Si, introduces tensile strains in the lattice and tend to associate with self-interstitials. Notably, isovalent dopants in Si are widely used for defect engineering in Czochralski silicon (Cz-Si) [10–14].

Aside from oxygen, carbon is an important impurity in Si unintentionally added during material growth [1,9,15,16]. In previous studies, the interactions of C with self-interstitials and various impurities have been reported to mainly be with O and other C atoms, leading to families of (C–O)-related (for instance,  $C_iO_i$ ,  $C_iO_i(Si_i)_n$ ) [9,16–20] and C-related defects (for instance,  $C_iC_s$ ,  $C_iC_s(Si_i)_n$ ) [9,16,21–24]. Notably, carbon affects oxygen precipitation [25,26] in Si. Also, carbon co-doping in doped Si suppresses the formation of boron–oxygen complexes, which is very important for the performance of crystalline Si solar cells [27].

Ge, when introduced into the Si lattice, affects the properties of Si in many ways. It has been found that Ge atoms, by locking dislocations, can enhance the mechanical strength of Si, which improves the production yield of the material [28,29]. It suppresses thermal donors, which stabilizes the electrical properties of Si [30]. It enhances oxygen precipitation and improves the internal gettering capability of metallic contamination which is very important for device fabrication [31,32]. It suppresses void defects and thus offers high quality polished surface for epi-layer growth in Si [33]. It suppresses the formation of large-sized crystals originated particles (COPs), thereby improving the quality of the surface of the material for epitaxial growth [34]. Ge also suppresses B–O defects that lead to light-induced degradation (LID) of carrier lifetime, which is an important issue for the solar cells industry [35]. Importantly, Ge affects the production and evolution of O-related and C-related irradiation induced defects in Si [36–38]. Ge-doping is a valuable technique to control the formation and the thermal stability of O-related and C-related defects in Si. Interestingly, co-doping has proven to be a promising strategy for effectively tuning the electrical, mechanical, and optical properties of semiconductors, particularly Si. [10,36,39,40]. Central to this co-doping of Si with Ge and C, ( $r_{Ge} > r_{Si}$ , although  $r_C < r_{Si}$ ) is a complementary strategy to enhance device operation through controlling defect properties. It has been determined that the simultaneous Ge and C co-doping improves radiation hardness of the Cz-Si substrate [12,41]. Moreover, Ge and C co-doping has been found to suppress the large-size voids in Si which generate leakage currents that deteriorate the efficiency of electronic devices [10,40].

Sn is also an important isovalent dopant impurity in Si. Sn, being larger than the Si atom, attracts vacancies thus reducing the formation of VO and  $VO_2$  defects in Si [42–44]. This tendency to attract vacancies promotes Sn as a promising dopant for radiation hardness in Si [45]. Additionally, the large Sn atoms are used to compensate strain layers in B-doped Si, which is the basic substrate material for power devices [46]. Since Sn attracts vacancies and C attracts self-interstitials, it has been proposed that Sn and C co-doping in Si could further enhance the radiation hardening potential of the material [42,47], which is valuable for application with solar cells and detectors operating in radiation environments [48]. Furthermore, since the introduction of C, which is a small atom compared to Si, contracts the lattice when introduced at substitutional sites, as opposed to the case of Sn which is larger than Si and expands the lattice, the compensation for each other's strains could effectively enhance their solubility [49]. This is important for the fabrication of carbon-implanted light-emitted diodes [46,49]. This also raises an interest for any possible interaction between Sn and C and the formation of Sn–C pairs. Thus, Sn and C co-doping was proposed as a tool to assess the degradation of Si-based devices [42].

Lead has an even larger covalent radius than Sn and the consequence is that there is an introduction of significant strains in the lattice that can affect the equilibrium concentrations and defect processes involving intrinsic defects [50,51]. Regarding radiation defects, Pb doping can affect the production evolution and the reactions of various  $V_nO$  and  $VO_m$  defects in Si, indicating a practical interest for defect engineering [52–55]. Notably, Pb in Si does not introduce any levels in the forbidden gap in comparison with Sn [52]. Additionally, when Pb and C are simultaneously in the lattice, the compressive strains introduced by Pb can be compensated by the tensile strains introduced by C. Technically, co-doping with C and Pb has been used to stabilize Pb at substitutional sites and suppress

its precipitation [52,56]. It is therefore of interest to investigate the interaction between Pb and C for the formation of carbon–lead pairs [14].

Among the Ge–C, Sn–C, and Pb–C pairs, it is worth noting that only Sn–C has been studied more thoroughly, both experimentally and theoretically [47,57–59]. A number of IR lines at 873, 1025.3, and 6875  $\text{cm}^{-1}$  were attributed [47] to the  $(\text{C}_i\text{Sn}_s)^{2N}$  with  $\text{C}_i$  at the second neighboring position, with respect to the Sn. Additional lines at 888.9, 985.3 and 6915  $\text{cm}^{-1}$  were also attributed to a less stable  $\text{C}_i\text{Sn}_s)^{2N*}$  configuration [58]. Regarding the Ge–C and Pb–C pairs, their presence were proposed theoretically and was indirectly concluded experimentally from variations in the concentrations of the O and C-related defects [14,60,61].

Isovalent doping in Si is a valuable technique used to optimize devices. In particular, Ge, Sn, and Pb, when present in the Si lattice, affect the formation, the concentration, thermal stability, and reactions of the oxygen-related and C-related defects. This is important for the radiation hardness of the material, especially when Si-based devices such as detectors are operated in radiation environments. Ge, Sn, and Pb co-doping with C is also a practical way to improve the defect reactions and processes in silicon. Here, we have employed DFT calculations to study the Ge–C, Sn–C, and Pb–C pairs in Si. In particular, the focus is on the impact of the dopant size on the stability of the defect pair and whether substitutional or interstitial dopants will produce more energetically favorable defect pairs. The criterion considered here is binding energy.

## 2. Computational Methodology

We used a plane-wave DFT code implemented in the Cambridge Serial Total Energy Package (CASTEP) to perform all the calculations [62,63]. Taking into account the exchange–correlation interactions, we used the Generalized Gradient Approximation (GGA) method with ultrasoft pseudopotentials [64] to depict the electron–ion interactions [65]. For the bulk Si structure, we used a 250 atoms’ supercell. A  $2 \times 2 \times 2$  Monkhorst–Pack k-point grid [66] was used and the cut-off energy was 350 eV. For the structures’ optimization, we used the Broyden–Fletcher–Goldfarb–Shanno (BFGS) geometry optimization method [67,68]. We used a step-by-step approach, performing more than 30 calculations for each defect (Ge, Sn, Pb) for both the  $\text{C}_i$  and  $\text{C}_s$  formations until the lowest energy structure was reached in each case. We used the Defects and Impurities Setup (DIMS) tool [69] to automate the process and to avoid possible mistakes that arise from setting up the calculations by hand. The figures in this paper were produced using the Visualization for Electronic and Structural Analysis (VESTA) software (v 3) [70].

## 3. Results

### 3.1. Carbon Substitutional-Isovalent Dopant Defect Pairs

The Ge atoms in the Si lattice are completely soluble and can form  $\text{Si}_{1-x}\text{Ge}_x$  alloys [71]. Conversely, the larger Sn and Pb are not completely soluble over the compositional range but only for a limited range (i.e., for small Sn and Pb compositions) [72]. The incorporation of isovalent dopant atoms is important as they can modify the optical, electronic, and structural properties [71,72].

Figure 1 represents the energetically favorable carbon substitutional-isovalent dopant substitutional  $\text{C}_s\text{D}_s$  ( $\text{D} = \text{Ge}, \text{Sn}, \text{Pb}$ ) defects. These were derived using DFT calculations for all the possible configurations within the supercell. Here, the binding energy (i.e., energy of the defect pair minus the energy of the isolated constituent defects) is the measure of stability. The binding energy of a  $\text{C}_s\text{D}_s$  defect can be calculated using the following equation:

$$E_b(\text{C}_s\text{D}_s) = E_{\text{C}_s\text{D}_s\text{-supercell}} + E_{\text{Si-supercell}} - E_{\text{C}_s\bullet\text{Si-supercell}} - E_{\text{D}_s\text{-supercell}} \quad (1)$$

where  $E_{\text{C}_s\text{D}_s\text{-supercell}}$  is the total energy of a Si supercell containing a  $\text{C}_s\text{D}_s$  defect,  $E_{\text{Si-supercell}}$  is the total energy of a Si supercell,  $E_{\text{C}_s\bullet\text{Si-supercell}}$  is the total energy of the Si supercell containing a C substitutional, and  $E_{\text{D}_s\bullet\text{Si-supercell}}$  is the total energy of the Si supercell containing a D substitutional.

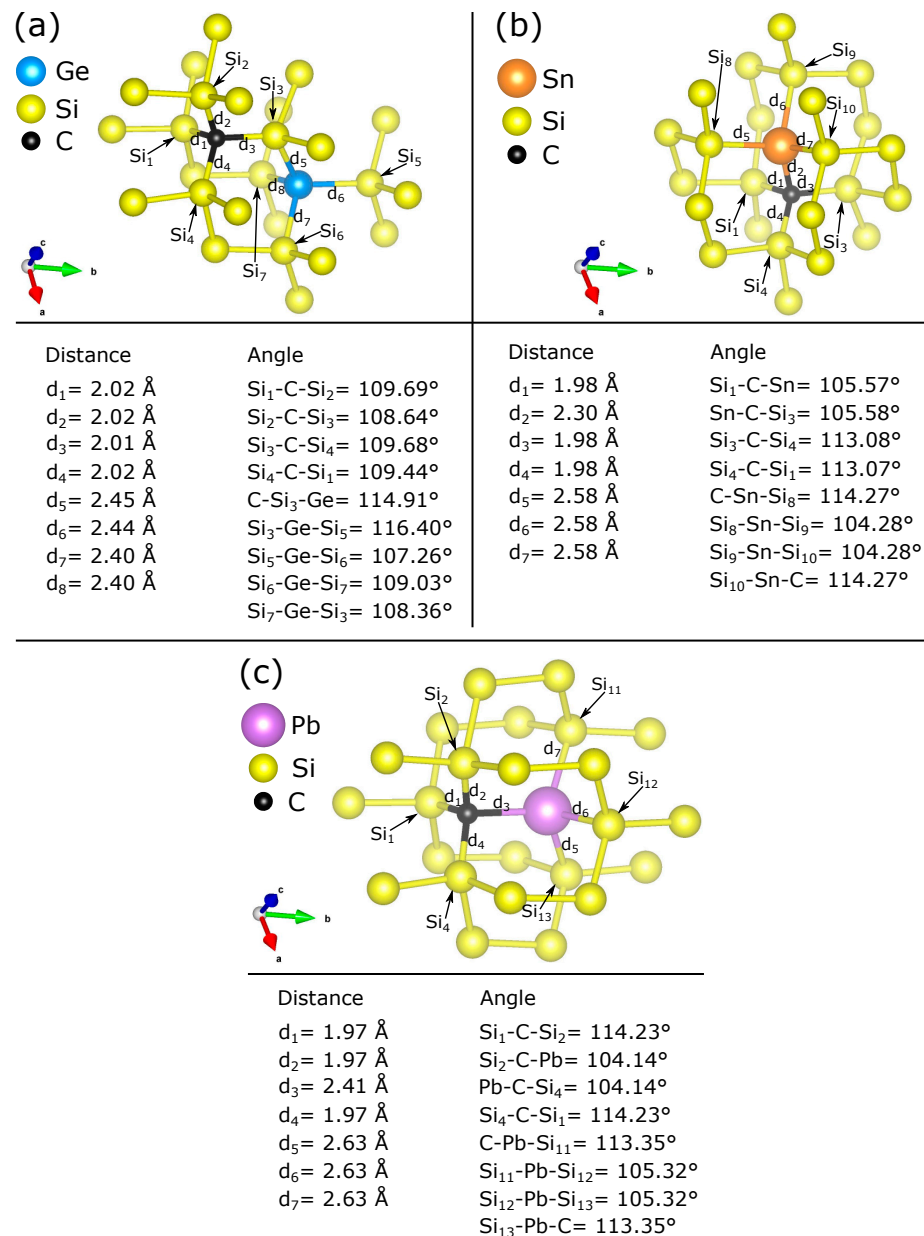


**Figure 1.** Schematic representation of the energetically favorable (a)  $C_5Ge_5$ , (b)  $C_5Sn_5$  and (c)  $C_5Pb_5$  defects in Si. Important distances and angles in the vicinity of the defects are given. Dimmer atoms represent atoms in the background.

The electronegativity difference between the C substitutional and the Si lattice atoms is reflected in the shorter Si–C as compared to the Si–Si (or Si–D) bond distances (refer to Figure 1). It should be stressed at this point that the distances and bond angles are given in both Figures 1 and 2 in order to facilitate a comparison, as well as for other scientists to facilitate a comparison with their results in the future and to consider whether they have reproduced the present results or found alternative geometries.

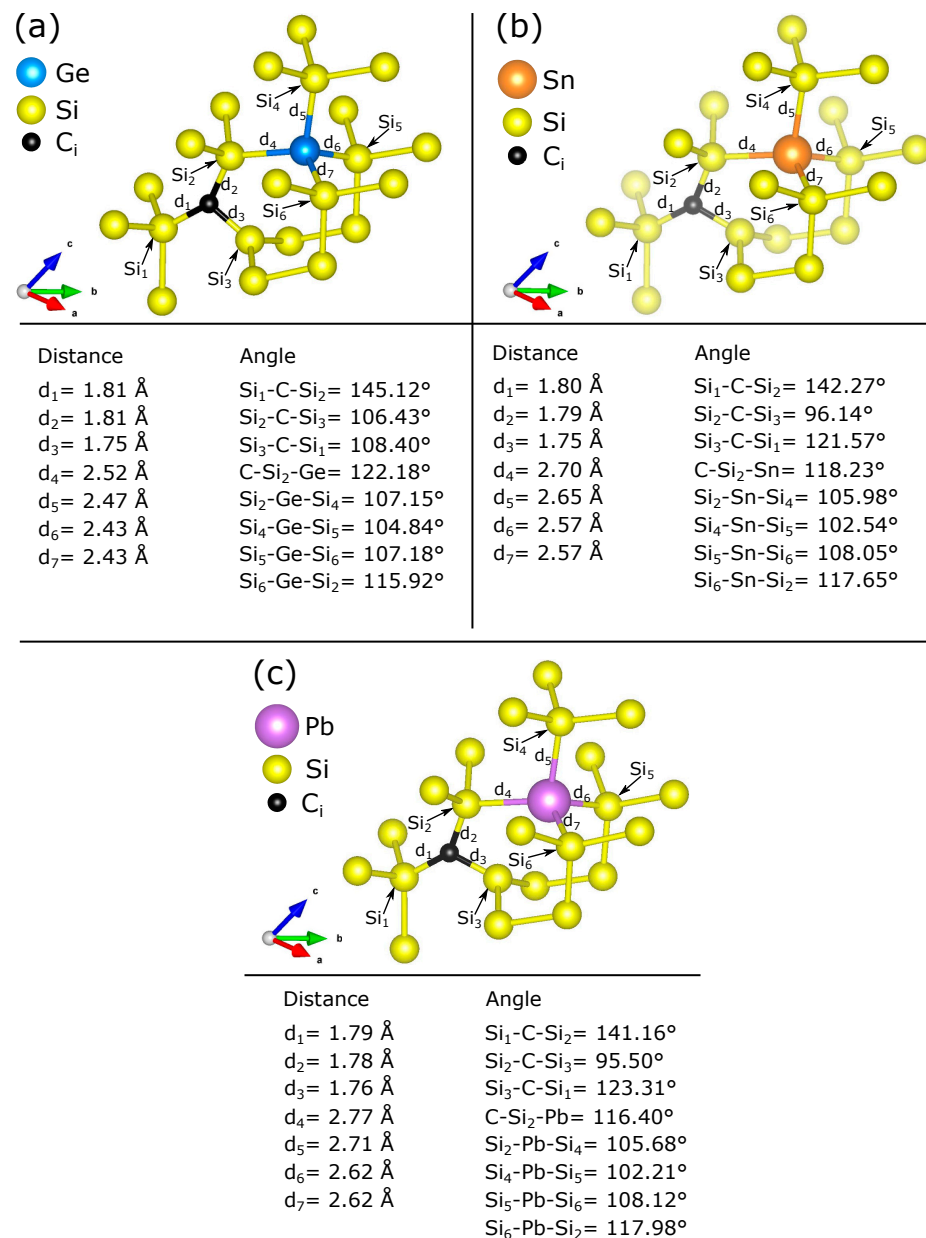


**Figure 2.** Schematic representation of the energetically favorable (a)  $\text{C}_1\text{GeS}_5$ , (b)  $\text{C}_1\text{SnS}_5$  and (c)  $\text{C}_1\text{PbS}_5$  defects in Si. Important distances and angles in the vicinity of the defects are given. Dimmer atoms represent atoms in the background.

The  $\text{C}_5\text{GeS}_5$  pair is only weakly bound (by  $-0.10 \text{ eV}$ ) and forms when the C atom is at the second nearest neighbor configuration as compared to Sn (refer to Figure 1). Conversely, in both the  $\text{C}_5\text{SnS}_5$  and  $\text{C}_5\text{PbS}_5$  defects, the isovalent atom is at nearest neighbor sites with respect to the C atom (refer to Figure 1). The  $\text{C}_5\text{SnS}_5$  pair was calculated to be bound by  $-0.42 \text{ eV}$  in good agreement with previous theoretical studies ( $-0.19$  to  $-0.20 \text{ eV}$ , [47,73]). The  $\text{C}_5\text{PbS}_5$  pair is bound more ( $-0.56 \text{ eV}$ ) as the larger Pb atom takes more advantage of the space provided by the smaller (compared to Si) carbon substitutional atom.

### 3.2. Carbon Interstitial-Isovalent Dopant Defect Pairs

The carbon atoms in the Si lattice can also reside in interstitial positions. Figure 2 represents the energetically favorable carbon interstitial-isovalent dopant substitutional



$C_iD_s$  ( $D = \text{Ge, Sn, Pb}$ ) defects. The binding energy of a  $C_iD_s$  defect can be calculated using the following equation:

$$E_b(C_iD) = E_{C_iD_s\text{-supercell}} + E_{\text{Si-supercell}} - E_{C_i\bullet\text{Si-supercell}} - E_{D_s\text{-supercell}} \quad (2)$$

where  $E_{C_iD_s\text{-supercell}}$  is the total energy of a Si supercell containing a  $C_iD_s$  defect and  $E_{C_i\bullet\text{Si-supercell}}$  is the total energy of the Si supercell containing a  $C_i$ .

The energetically favorable  $C_iD_s$  defects were derived using DFT calculations for all the possible carbon interstitial configurations in the vicinity of the D substitutional within the supercell. The repulsion of larger isovalent dopants with interstitials is due to the local distortion of the oversized isovalent atoms that effectively limits the space that is required for the interstitial  $C_i$  defects.

Figure 3 summarizes the dependence on the isovalent dopant radius on the carbon-dopant binding energies. The isovalent dopant radius is a key criterion, given that the lattice is locally strained by the introduction of the dopant. These local strains contribute significantly to binding energies, particularly in defect clusters consisting of isovalent dopants where there is no contribution from the dopant charge states. In that sense, the dopant radius is a common criterion used to discuss energetics of defect clusters. The main trend of this figure is that the larger the dopant, the more stable the defect pair (i.e., more negative binding energy). Also, it is clear that the  $C_sD_s$  defects are more bound than the  $C_iD_s$  defects.

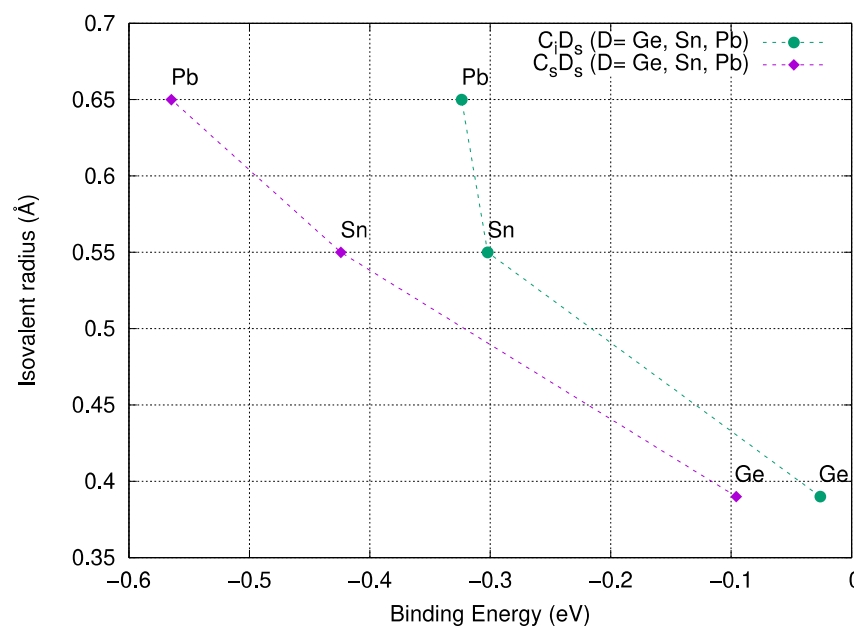


**Figure 3.** The impact of the isovalent dopant radius on the binding energy of the  $C_sD_s$  and  $C_iD_s$  (where  $D_s = \text{Ge, Sn, Pb}$ ) pairs in Si.

#### 4. Discussion

C can exist in considerable concentrations in Cz-silicon. Nevertheless, the formation of  $C_sD_s$  and  $C_iD_s$  defects will rely also on the D content and the kinetics. If there is significant variation in temperature and pressure or limited experimental data, the study of the kinetics will benefit from the cBΩ thermodynamic model [74,75] and this has been employed to Si and related systems [76,77].

Considering the  $C_sD_s$  and  $C_iD_s$  (where  $D_s = \text{Ge, Sn, Pb}$ ) pairs studied here as compared to analogous carbon-related defects encountered in Cz-Si (for example, [19,78] and references therein). It is known that in Cz-Si, there exists a significant carbon and oxygen concentration introduced during crystal growth [15,16]. If we also consider the processing conditions, intrinsic point defects will also form and therefore the formation of the  $C_sD_s$

and  $C_iD_s$  defect pairs considered here will be antagonistic to defects such as  $C_sC_s$ ,  $C_iO_i$ , etc. Putting aside kinetic considerations and assuming that all defects have pathways to form and are not hindered by kinetics, the criterion that can be used for the prevalence of specific defect species would be binding energies. In this line of thought, a strongly negative binding energy will denote that a defect pair will be more likely to form as compared to a less bound defect pair. For example, a migrating  $C_i$  defect will be more easily captured by an oxygen interstitial (binding energy  $-1.6$  eV) [19] than an isovalent dopant atom (refer to Table 1). This, of course, will assume that the initial concentrations of defects will be equal as the law of mass action will favor defects with higher initial concentrations of defects. It can be seen from Table 1 that the capture efficiency (based solely on binding energies) of the defect pairs considered here is far less important than competitive carbon-containing defect pairs. Therefore, the isovalent dopant-containing pairs will be far less populous and can only play a role if there is a high content of isovalent dopants and hence, a higher probability of the migrating carbon atoms to reach them and be attracted by them at nearest neighbor sites.

**Table 1.** The binding energies of carbon-related defect pairs in Si.

Defect	Binding Energy/eV	Comments
$C_i(Si_I)$	$-2.34$	Ref. [19]
$C_iO_i$	$-1.6$	Ref. [19]
$C_iC_s$	$-1.68$	Ref. [19]
$C_sGe_s$	$-0.10$	present study
$C_sSn_s$	$-0.42$	present study
$C_sPb_s$	$-0.56$	present study
$C_iGe_s$	$-0.03$	present study
$C_iSn_s$	$-0.30$	present study
$C_iPb_s$	$-0.32$	present study

## 5. Conclusions

Here, we considered the structure and formation of carbon-isovalent defects in Si, which is scientifically and technologically important. We employed DFT calculations to provide detailed information on the structure of carbon-isovalent substitutional pairs, where the carbon atom resides at a substitutional or an interstitial site in the Si lattice. The main conclusion is that the larger the dopant, the more stable the defect pair. Additionally, for all the cases considered, the  $C_sD_s$  defects are more bound than the  $C_iD_s$  defects. Here the criterion is binding energies, and we did not consider in detail the formation of these defects. Using DFT calculations, we characterized the geometry (bond lengths and angles) of all the defect pairs considered, aiming to provide information to future experimental and theoretical studies. It is anticipated that the present study can be the basis for future experimental and theoretical work on this system and, in particular, the kinetics to form the extended C-related defects. In essence, the present work can serve as a paradigm that can be used in a transferable manner to investigate carbon-dopant and related defects in semiconducting systems.

**Author Contributions:** Formal analysis, S.-R.G.C., E.N.S. and A.C.; Investigation, C.A.L. The manuscript was written and edited by all authors. All authors have read and agreed to the published version of the manuscript.

**Funding:** This research received no external funding.

**Data Availability Statement:** Data is contained within the article.

**Conflicts of Interest:** The authors declare no conflicts of interest.

## References

1. Yang, D. (Ed.) *Handbook of Photovoltaic Silicon*; Springer: Berlin/Heidelberg, Germany, 2019.
2. Udvarhelyi, P.; Somogyi, B.; Thiering, G.; Gali, A. Identification of a Telecom Wavelength Single Photon Emitter in Silicon. *Phys. Rev. Lett.* **2021**, *127*, 196402. [\[CrossRef\]](#)
3. Liu, W.; Ivanov, V.; Jhuria, K.; Ji, Q.; Persaud, A.; Redjem, W.; Simoni, J.; Zhiyenbayev, Y.; Kante, B.; Lopez, J.G.; et al. Quantum Emitter Formation Dynamics and Probing of Radiation-Induced Atomic Disorder in Silicon. *Phys. Rev. Appl.* **2023**, *20*, 014058. [\[CrossRef\]](#)
4. Bisogni, M.G.; Del Guerra, A.; Belcari, N. Medical applications of silicon photomultipliers. *Nucl. Inst. Methods Phys. Res. A* **2019**, *926*, 118–128. [\[CrossRef\]](#)
5. Jia, X.; He, L. Noise-based analysis of the reliability of silicon solar cells. *AIP Adv.* **2021**, *11*, 045206. [\[CrossRef\]](#)
6. Freysoldt, C.; Grabowski, B.; Hichel, T.; Neugebauer, J.; Janotti, G.; van de Walle, G. First-principles calculations for point defects in solids. *Rev. Mod. Phys.* **2014**, *86*, 253–305. [\[CrossRef\]](#)
7. McCluskey, M.D.; Jannotti, A. Defects in Semiconductors. *J. Appl. Phys.* **2020**, *127*, 190401. [\[CrossRef\]](#)
8. Drabold, D.A.; Estreicher, S.K. (Eds.) *Theory of Defects in Semiconductors*; Topics in Applied Physics; Springer: Berlin/Heidelberg, Germany, 2007; Volume 14.
9. Pichler, P. *Intrinsic Point Defects, Impurities, and Their Diffusion in Silicon*; Springer: Wien, Austria, 2004.
10. Yu, X.; Chen, J.; Ma, X.; Yang, D. Impurity engineering of Czochralski silicon. *Mater. Sci. Eng. R* **2013**, *74*, 1–33. [\[CrossRef\]](#)
11. Chen, J.; Yang, D. Impurity engineering for germanium-doped Czochralski silicon wafer used for ultra-large scale integrated circuit. *Phys. Stat. Sol. C* **2009**, *6*, 625. [\[CrossRef\]](#)
12. Londos, C.A.; Andrianakis, A.; Emtsev, V.V.; Ohyama, H. Radiation-induced defects in Czochralski-grown silicon containing carbon and germanium. *Semicond. Sci. Technol.* **2009**, *24*, 075002. [\[CrossRef\]](#)
13. Chroneos, A.; Londos, C.A.; Sgourou, E.N.; Pochet, P. Point defect engineering strategies to suppress A-center formation in silicon. *Appl. Phys. Lett.* **2011**, *99*, 241901. [\[CrossRef\]](#)
14. Sgourou, E.N.; Timerkaeva, D.; Londos, C.A.; Aliprantis, D.; Chroneos, A.; Calliste, D.; Pochet, P. Impact of isovalent doping on the trapping of vacancy and interstitial related defects in Si. *J. Appl. Phys.* **2013**, *113*, 113506. [\[CrossRef\]](#)
15. Newman, R.C. Oxygen, Carbon, Hydrogen and Nitrogen in Crystalline Silicon. In Proceedings of the Materials Research Society Symposia Proceedings, Boston, MA, USA, 2–5 December 1985; Mikkelsen, J.C., Jr., Pearton, S.J., Corbett, J.W., Pennycook, S.J., Eds.; 1986; Volume 59, p. 403.
16. Davies, G.; Newman, R.C. Carbon in Crystalline Silicon. In *Handbook on Semiconductors*; Mahajan, S., Ed.; Elsevier Science B.V.: Amsterdam, The Netherlands, 1994; Volume 3, p. 1557.
17. Londos, C.A.; Sgourou, E.N.; Chroneos, A.; Emtsev, V.V. Carbon, oxygen and intrinsic defect interactions in germanium-doped silicon. *Semicond. Sci. Technol.* **2011**, *26*, 105024. [\[CrossRef\]](#)
18. Londos, C.A.; Aliprantis, D.N.; Antonaras, G.; Potsidi, M.S.; Angeletos, T. Experimental and theoretical study of the C<sub>4</sub> defect in neutron irradiated silicon. *J. Appl. Phys.* **2018**, *123*, 145702. [\[CrossRef\]](#)
19. Wang, H.; Chroneos, A.; Londos, C.A.; Sgourou, E.N.; Schwingenschlogl, U. Carbon related defects in irradiated silicon revisited. *Sci. Rep.* **2014**, *4*, 4909. [\[CrossRef\]](#) [\[PubMed\]](#)
20. Potsidi, M.S.; Kuganathan, N.; Chroneos, A.; Christopoulos, S.-R.G.; Angeletos, T.; Sarlis, N.V.; Londos, C.A. Substitutional carbon-dioxygen center in irradiated silicon. *Mater. Sci. Semicond. Proc.* **2021**, *127*, 105661. [\[CrossRef\]](#)
21. Wang, H.; Chroneos, A.; Londos, C.A.; Sgourou, E.N.; Schwingenschlogl, U. G-centers in irradiated silicon revisited: A screened hybrid density functional theory approach. *J. Appl. Phys.* **2014**, *115*, 183523. [\[CrossRef\]](#)
22. Potsidi, M.; Londos, C.A. The C<sub>1</sub>C<sub>5</sub>(S<sub>II</sub>) defect in silicon: An infrared spectroscopy study. *J. Appl. Phys.* **2006**, *100*, 033523. [\[CrossRef\]](#)
23. Londos, C.A.; Chroneos, A.; Sgourou, E.N.; Panagiotidis, I.; Angeletos, T.; Potsidi, M.S. Comparative Study of Oxygen- and Carbon-Related Defects in Electron Irradiated Cz-Si Doped with Isovalent Impurities. *Appl. Sci.* **2022**, *12*, 8151. [\[CrossRef\]](#)
24. Deak, P.; Udvarhelyi, P.; Thiering, G.; Smith, A. The kinetics of carbon pair formation in silicon prohibits reaching thermal equilibrium. *Nat. Commun.* **2023**, *14*, 361. [\[CrossRef\]](#)
25. Tan, T.Y.; Taylor, W.J. Mechanisms of Oxygen precipitation: Some quantitative aspects, in Oxygen in Silicon. In *Semiconductor and Semimetals*; Shimura, F., Ed.; Springer: Berlin/Heidelberg, Germany, 1994; Volume 42, pp. 353–390.
26. Kissinger, G. Oxygen Impurity in Crystalline Silicon. In *Handbook of Photovoltaic Silicon*; Yang, D., Ed.; Springer: Berlin/Heidelberg, Germany, 2019.
27. Wu, Y.; Yunn, S.; Qiu, X.; Zhu, H.; Qian, J.; Yang, D. Impact of carbon co-doping on the performance of crystalline silicon solar cells. *Sol. Energy Mater. Sol. Cells* **2016**, *154*, 94. [\[CrossRef\]](#)
28. Taishi, T.; Huang, X.; Yonenaga, I.; Hashikawa, K. Dislocation behavior in heavily germanium-doped silicon crystal. *Mater. Sci. Semicond. Process.* **2002**, *5*, 409–412. [\[CrossRef\]](#)
29. Chen, J.; Yang, D.; Ma, X.; Zeng, Z.; Tian, D.; Li, L.; Que, D.; Gong, L. Influence of germanium doping on the mechanical strength of Czochralski silicon wafers. *J. Appl. Phys.* **2008**, *103*, 123521. [\[CrossRef\]](#)
30. Dashevskii, M.Y.; Dokuchaeva, A.A.; Sadilov, S.I. On the solubility of oxygen in silicon doped with germanium. *Inorg. Mater.* **1989**, *25*, 580.



31. Chen, J.; Yang, D.; Li, H.; Ma, X.; Que, D. Enhancement effect of germanium on oxygen precipitation in Czochralski silicon. *J. Appl. Phys.* **2006**, *99*, 073509. [\[CrossRef\]](#)
32. Chen, J.; Yang, D.; Ma, X.; Que, D. Rapid-thermal-anneal-based internal gettering for germanium-doped Czochralski silicon. *Appl. Phys. A* **2009**, *94*, 905–910. [\[CrossRef\]](#)
33. Carbonaro, C.M.; Fiorentini, V.; Bernardini, F. Stability of Ge-related point defects and complexes in Ge-doped SiO<sub>2</sub>. *Phys. Rev. B* **2002**, *66*, 233201. [\[CrossRef\]](#)
34. Chen, J.; Yang, D.; Li, H.; Ma, X.; Tian, D.; Li, L.; Que, D. Crystal-originated particles in germanium-doped Czochralski silicon crystal. *J. Cryst. Growth* **2007**, *306*, 262–268. [\[CrossRef\]](#)
35. Wang, P.; Yu, X.; Chen, P.; Li, X.; Yang, D.; Chen, X.; Huang, Z. Germanium-doped Czochralski silicon for photovoltaic applications. *Sol. Energy Mater. Sol. Cells* **2011**, *95*, 2466. [\[CrossRef\]](#)
36. Chroneos, A.; Sgourou, E.N.; Londos, C.A.; Schwingenschlogl, U. Oxygen defect processes in silicon and silicon germanium. *Appl. Phys. Rev.* **2015**, *2*, 021306. [\[CrossRef\]](#)
37. Londos, C.A.; Andrianakis, A.; Sgourou, E.N.; Emtsev, V.; Ohyama, H. Effect of germanium doping on the annealing characteristics of oxygen and carbon-related defects in Czochralski silicon. *J. Appl. Phys.* **2010**, *107*, 093520. [\[CrossRef\]](#)
38. Voronkov, V.V.; Falster, R.; Londos, C.A.; Sgourou, E.N.; Andrianakis, A.; Ohyama, H. Production of vacancy-oxygen defect in electron irradiated silicon in the presence of self-interstitial-trapping impurities. *J. Appl. Phys.* **2011**, *110*, 093510. [\[CrossRef\]](#)
39. Zhang, J.; Tse, K.; Wong, M.; Zhang, Y.; Zhu, J. A brief review of co-doping. *Front. Phys.* **2016**, *11*, 117405. [\[CrossRef\]](#)
40. Londos, C.A.; Sgourou, E.N.; Hall, D.; Chroneos, A. Vacancy-oxygen defects in silicon: The impact of isovalent doping. *J. Mater. Sci. Mater. Electron.* **2014**, *25*, 2395–2410. [\[CrossRef\]](#)
41. Londos, C.A.; Andrianakis, A.; Sgourou, E.N.; Emtsev, V.V.; Ohyama, H. IR studies of the impact of Ge doping on the successive conversion of Von defects in Czochralski-Si containing carbon. *J. Appl. Phys.* **2009**, *105*, 123508. [\[CrossRef\]](#)
42. Brelot, A. Tin as a Vacancy Trap in Silicon at Room Temperature. *IEEE Trans. Nucl. Sci.* **1972**, *19*, 220–223. [\[CrossRef\]](#)
43. Watkins, G.D. Defects in irradiated silicon: EPR of the tin-vacancy pair. *Phys. Rev. B* **1975**, *12*, 4383. [\[CrossRef\]](#)
44. Chroneos, A.; Londos, C.A.; Sgourou, E.N. Effect of tin doping on oxygen- and carbon-related defects in Czochralski silicon. *J. Appl. Phys.* **2011**, *110*, 093507. [\[CrossRef\]](#)
45. Chroneos, A.; Londos, C.A. Interaction of A-centers with isovalent impurities in silicon. *J. Appl. Phys.* **2010**, *107*, 093518. [\[CrossRef\]](#)
46. Clays, C.; Simoen, E.; Neimash, V.B.; Kraitchinskii, A.; Krasko, M.; Puzenko, O.; Blondeel, A.; Clauws, P. Tin Doping of Silicon for Controlling Oxygen Precipitation and Radiation Hardness. *J. Electrochem. Soc.* **2001**, *148*, G738. [\[CrossRef\]](#)
47. Lavrov, E.V.; Fanciully, M.; Kaukonen, M.; Jones, R.; Briddon, P.R. Carbon-tin defects in silicon. *Phys. Rev. B* **2001**, *64*, 125212. [\[CrossRef\]](#)
48. Linstrom, G.; Moll, M.; Fretwurst, E. Radiation hardness of silicon detectors—A challenge from high-energy physics. *Nucl. Instrum. Meth. Phys. Res. A* **1999**, *426*, 1–15. [\[CrossRef\]](#)
49. Canham, L.T.; Dyball, M.R.; Barraclough, K.G. A study of carbon-implanted silicon for light-emitting diode fabrication. *Mater. Sci. Eng. B* **1989**, *4*, 95. [\[CrossRef\]](#)
50. Caliste, D.; Rushchanskii, K.Z.; Pochet, P. Vacancy-mediated diffusion in biaxially strained Si. *Appl. Phys. Lett.* **2011**, *98*, 031908. [\[CrossRef\]](#)
51. Chroneos, A.; Jiang, C.; Grimes, R.W.; Schwingenschlöggl, U.; Bracht, H. E centers in ternary Si<sub>1-x</sub>-yGe<sub>x</sub>Sny random alloys. *Appl. Phys. Lett.* **2009**, *95*, 112101. [\[CrossRef\]](#)
52. David, M.L.; Simoen, E.; Clays, C.; Neimash, V.B.; Krasko, M.; Kraitchinskii, A.; Voytovych, V.; Kabaldin, A.; Barbot, J.F.J. Electrically active defects in irradiated n-type Czochralski silicon doped with group IV impurities. *Phys. Condens. Mater.* **2005**, *17*, S2255. [\[CrossRef\]](#)
53. Neimash, V.B.; Voytovych, V.V.; Kras'ko, M.; Kraitchinskii, A.M.; Kabaldin, O.M.; Pavlos'kyi, Y.V.; Tsmots', V.M. Formation of Radiation-induced Defects in n-Si with Lead and Carbon Impurities. *Ukr. J. Phys.* **2005**, *50*, 1273.
54. Londos, C.A.; Aliprantis, D.N.; Sgourou, E.N.; Chroneos, A.; Pochet, P. Formation and evolution of oxygen-vacancy clusters in lead and tin doped silicon. *J. Appl. Phys.* **2012**, *111*, 123508. [\[CrossRef\]](#)
55. Londos, C.A.; Sgourou, E.N.; Chroneos, A. Defect engineering of the oxygen-vacancy clusters formation in electron irradiated silicon by isovalent doping: An infrared perspective. *J. Appl. Phys.* **2012**, *112*, 123517. [\[CrossRef\]](#)
56. Milants, K.; Verheyden, J.; Balancira, T.; Dewerd, W.; Pattyn, H.; Bukshpan, S.; Williamson, D.L.; Vermeiren, F.; van Tandeloo, G.; Viakken, C.; et al. Size distribution and magnetic behavior of lead inclusions in silicon single crystals. *J. Appl. Phys.* **1997**, *81*, 2148. [\[CrossRef\]](#)
57. Lavrov, E.V.; Fanciully, M. Interstitial carbon-substitutional tin center in silicon (?). *Phys. B. Condens. Matter* **2001**, *302–303*, 263. [\[CrossRef\]](#)
58. Khirunen, L.I.; Kobzar, O.O.; Pomozov, Y.V.; Sosnin, M.G.; Tripachko, M.O.; Abrosimov, N.V.; Riemann, H. Interstitial-related reactions in silicon doped with isovalent impurities. *Phys. B Condens. Matter* **2003**, *340*, 546. [\[CrossRef\]](#)
59. Khirunen, L.I.; Kobzar', O.A.; Pomozov, Y.V.; Sosnin, M.G.; Tripachko, N.A. The role of tin in reactions involving carbon interstitial atoms in irradiated silicon. *Semiconductors* **2003**, *37*, 288. [\[CrossRef\]](#)
60. Londos, C.A.; Sgourou, E.N.; Timerkaeva, D.; Chroneos, A.; Emtsev, V.V. Impact of isovalent doping on radiation defects in silicon. *J. Appl. Phys.* **2013**, *114*, 113504. [\[CrossRef\]](#)

61. Londos, C.A.; Angeletos, T.; Sgourou, E.N.; Chroneos, A. Engineering VO, E, C<sub>i</sub>O<sub>i</sub> and C<sub>i</sub>C<sub>s</sub> defects in irradiated Si through Ge and Pb doping. *J. Mater. Sci. Mater. Electron.* **2015**, *26*, 2248. [\[CrossRef\]](#)
62. Payne, M.C.; Teter, M.P.; Allan, D.C.; Arias, T.A.; Joannopoulos, J.D. Iterative minimization techniques for ab initio total-energy calculations: Molecular dynamics and conjugate gradients. *Rev. Mod. Phys.* **1992**, *64*, 1045. [\[CrossRef\]](#)
63. Clark, S.J.; Segall, M.D.; Pickard, C.J.; Hasnip, P.J.; Probert, M.I.J.; Refson, K.; Payne, M.C. First principles methods using CASTEP. *Z. Krist.* **2005**, *220*, 567–570. [\[CrossRef\]](#)
64. Vanderbilt, D. Soft self-consistent pseudopotentials in a generalized eigenvalue formalism. *Phys. Rev. B* **1990**, *41*, 7892–7895. [\[CrossRef\]](#) [\[PubMed\]](#)
65. Wan, W.; Wang, H. First-Principles Investigation of Adsorption and Diffusion of Ions on Pristine, Defective and B-doped Graphene. *Materials* **2015**, *8*, 6163–6178. [\[CrossRef\]](#) [\[PubMed\]](#)
66. Monkhorst, H.J.; Pack, J.D. Special points for Brillouin-zone integrations. *Phys. Rev. B* **1976**, *13*, 5188. [\[CrossRef\]](#)
67. Pfrommer, B.G.; Côté, M.; Louie, S.G.; Cohen, M.L. Relaxation of Crystals with the Quasi-Newton Method. *J. Comp. Phys.* **1997**, *131*, 233–240. [\[CrossRef\]](#)
68. Packwood, D.; Kermode, J.; Mones, L.; Bernstein, N.; Woolley, J.; Gould, N.; Ortner, C.; Csányi, G.J. A universal preconditioner for simulating condensed phase materials. *Chem. Phys.* **2016**, *144*, 164109. [\[CrossRef\]](#)
69. Christopoulos, S.R.G.; Papadopoulou, K.A.; Konios, A.; Parfitt, D. DIMS: A tool for setting up defects and impurities CASTEP calculations. *Comp. Mater. Sci.* **2022**, *202*, 110976. [\[CrossRef\]](#)
70. Momma, K.; Izumi, F. VESTA 3 for Three-Dimensional Visualization of Crystal, Volumetric and Morphology Data. *J. Appl. Crystallogr.* **2011**, *44*, 1272–1276. [\[CrossRef\]](#)
71. Kube, R.; Bracht, H.; Chroneos, A.; Posselt, M.; Schmidt, B. Intrinsic and extrinsic diffusion of indium in germanium. *J. Appl. Phys.* **2009**, *106*, 063534. [\[CrossRef\]](#)
72. D’Costa, V.R.; Cook, C.S.; Menendez, J.; Tolle, J.; Kouvetakis, J.; Zollner, S. Transferability of optical bowing parameters between binary and ternary group-IV alloys. *Solid State Commun.* **2006**, *138*, 309. [\[CrossRef\]](#)
73. Chroneos, A. Isovalent impurity-vacancy complexes in germanium. *Phys. Stat. Sol. B* **2007**, *244*, 3206. [\[CrossRef\]](#)
74. Varotsos, P.; Alexopoulos, K. *Thermodynamics of Point Defects and Their Relation with the Bulk Properties*; Amelinckx, S., Gevers, R., Nihoul, J., Eds.; North Holland: Amsterdam, The Netherlands, 1986.
75. Varotsos, P.A.; Sarlis, N.V.; Skordas, E.S. Thermodynamics of Point Defects in Solids and Relation with the Bulk Properties: Recent Results. *Crystals* **2022**, *12*, 686. [\[CrossRef\]](#)
76. Cooper, M.W.D.; Grimes, R.W.; Fitzpatrick, M.E.; Chroneos, A. Modeling oxygen self-diffusion in UO<sub>2</sub> under pressure. *Solid State Ion.* **2015**, *282*, 26–30. [\[CrossRef\]](#)
77. Sarlis, N.V.; Skordas, E.S. Interconnection of a thermodynamical model for point defect parameters in solids with the dynamical theory of diffusion. *Solid State Ion.* **2019**, *335*, 82–85. [\[CrossRef\]](#)
78. Kuganathan, N.; Sgourou, E.N.; Chroneos, A.; Londos, C.A. The CsCs and CsCsV defects in silicon: Density functional theory calculations. *Silicon* **2024**, *16*, 703–709. [\[CrossRef\]](#)

**Disclaimer/Publisher’s Note:** The statements, opinions and data contained in all publications are solely those of the individual author(s) and contributor(s) and not of MDPI and/or the editor(s). MDPI and/or the editor(s) disclaim responsibility for any injury to people or property resulting from any ideas, methods, instructions or products referred to in the content.